PHYSICAL REVIEW B **94**, 115129 (2016)

Magnetic-field-induced spin crossover of Y-doped $Pr_{0.7}Ca_{0.3}CoO_3$

Akihiko Ikeda,[1,*] Suyeon Lee,[1] Taku T. Terashima,[1] Yasuhiro H. Matsuda,[1,†] Masashi Tokunaga,[1] and Tomoyuki Naito[2]
[1]*Institute for Solid State Physics, University of Tokyo, Kashiwa, Chiba 277-8581, Japan*
[2]*Faculty of Science and Engineering, Iwate University, Morioka, Iwate 020-8551, Japan*
(Received 7 July 2016; revised manuscript received 18 August 2016; published 13 September 2016)

The family of hole-doped Pr-based perovskite cobaltites, $Pr_{0.5}Ca_{0.5}CoO_3$ and $(Pr_{1-y}RE_y)_{0.3}Ca_{0.7}CoO_3$ (where RE is rare earth), has recently been found to exhibit simultaneous metal-insulator, spin-state, and valence transitions. We have investigated magnetic-field-induced phase transitions of $(Pr_{1-y}Y_y)_{0.7}Ca_{0.3}CoO_3$ by means of magnetization measurements at 4.2–100 K up to an ultrahigh magnetic field of 140 T with the chemical pressure varied by $y = 0.0625$, 0.075, 0.1. The observed magnetic-field-induced transitions were found to occur simultaneously with the metal-insulator transitions up to 100 T. The obtained magnetic-field-temperature (B-T) phase diagram and magnetization curves are well analyzed by a spin-crossover model of a single ion with interion interactions. On the other hand, the chemical pressure dependence of the experimentally obtained magnetization change during the phase transition disagrees with the single-ion model when approaching low temperatures. The significant y dependence of the magnetization change at low temperatures may arise from the itinerant magnetism of Co^{3+} in the paramagnetic metallic phase, where the chemical pressure enhances the exchange splitting by promoting the double-exchange interaction. The observed B-T phase diagrams of $(Pr_{1-y}Y_y)_{0.7}Ca_{0.3}CoO_3$ are quite contrary to that of $LaCoO_3$, indicating that in $(Pr_{1-y}Y_y)_{0.7}Ca_{0.3}CoO_3$ the high-field phase possesses higher entropy than the low-field phase, whereas it is the other way around in $LaCoO_3$.

DOI: 10.1103/PhysRevB.94.115129

I. INTRODUCTION

Strong correlations among electrons in transition-metal oxides often lead to the coupling of multiple degrees of freedom in solids, such as charge, orbital, and spin, that give rise to exotic phenomena such as superconductivity, colossal magnetoresistance, metal-insulator transition, multiferroics, and so forth. Cobaltites are considered unique among transition-metal oxides for their spin-state degrees of freedom. One of the most interesting phenomena expected in cobaltites is the ordering of spin states. A perovskite cobaltite, $LaCoO_3$, has been studied for over half a century. The spin states of octahedrally coordinated Co^{3+} ($3d^6$) are classified into low-spin (LS: $t_{2g}^6 e_g^0$), intermediated-spin (IS: $t_{2g}^5 e_g^1$), and high-spin (HS: $t_{2g}^4 e_g^2$) states according to their total spin angular momentum $S = 0$, 1, 2, respectively. Whereas the nonmagnetic and insulating ground state at $T < 30$ K in $LaCoO_3$ has been identified as the LS state with neutron scattering [1,2], its electronic excited state is still controversial. Various electronic energy schemes and ordered phases have been proposed, represented by the HS/LS order [3] and the uniform IS state with orbital order [4]. However, no such order or short-range correlations have been identified concretely by microscopic measures.

On the other hand, a hole-doped Pr-based perovskite cobaltite, $Pr_{0.5}Ca_{0.5}CoO_3$, was found to undergo the first-order and simultaneous magnetic, metal-insulator, and valence transitions [5]. The phase transition is considered analogous to the virtual phase change [6] between the ferromagnetic metallic phase of $La_{1-x}Sr_xCoO_3$ with $x > 0.3$ [7] and the diamagnetic insulator phase of $LaCoO_3$ at low temperatures [1]. The pressure and chemical pressure effects were found to be significant in $Pr_{1-x}Ca_xCoO_3$ with a small hole concentration ($x < 0.5$) [8–10]. The pressure suppresses the ferromagnetic order, and the paramagnetic insulator phase emerges [8,11]. The phase transition was claimed to be the spin-state transition between the Co^{3+} insulating LS state and metallic IS state [5,9]. Recent theoretical analyses of the two-orbital Hubbard model indicate the Bose-Einstein condensation of excitons is a possible origin of the insulating ground state of the Pr-based cobaltites [12–14].

In the last decade, studies employing high magnetic fields have revealed nontrivial field-induced phases of perovskite cobaltites. As for $LaCoO_3$, sharp first-order magnetic phase transitions are accompanied by large lattice expansions at around 60–65 T [15–17]. An even wider B-T phase diagram for $LaCoO_3$ has been constructed at high temperature up to 120 K and high magnetic fields up to 135 T [18]. The phase diagram revealed the two low-entropy phases emerge in the high-field region, which is counterintuitive to the single-ion picture. Rather, it indicates the presence of the inherent strong correlation between LS and HS or IS, which is debated theoretically [19,20]. On the other hand, for $(Pr_{1-y}Y_y)_{0.7}Ca_{0.3}CoO_3$, the B-T phase diagram has been revealed by magnetization and conductivity measurements for $y = 0.0625$ using static magnetic fields [21] and conductivity measurements for $y = 0.075$ and 0.1 using ultrahigh magnetic fields [22], where Y acts as the chemical pressure. Those studies commonly revealed the field-induced insulator-metal transitions. The transition fields decrease with increasing temperature, which is contrary to the case of $LaCoO_3$ [18] and more familiar among the spin-crossover systems in the single-ion picture [23,24].

In this paper, we present a high-field magnetization study of $(Pr_{1-y}Y_y)_{0.7}Ca_{0.3}CoO_3$ in a wide temperature range from 4.2 to 100 K and up to ultrahigh magnetic fields of 140 T, and the chemical pressure dependence is varied as $y = 0.0625$, 0.75, 0.1. A series of field-induced magnetic transitions

*ikeda@issp.u-tokyo.ac.jp
†ymatsuda@issp.u-tokyo.ac.jp

were observed. The obtained B-T phase diagrams are quite contrary to that of $LaCoO_3$, which is well analyzed with the spin-crossover model of a single ion from LS to IS induced by magnetic field. On the other hand, the amount of the magnetization change at the phase transitions was found to be too strongly dependent on the chemical pressure y to be explained by the above model. The possible origins of the discrepancy are discussed in terms of the itinerant magnetism of Co^{3+} in the IS state. Further, the vanishingly small latent heat at $y = 0.0625$ may suggest the presence of a critical point at low temperatures.

II. EXPERIMENT

Magnetization measurements $(Pr_{1-y}Y_y)_{0.7}Ca_{0.3}CoO_3$ for $y = 0.0625$, 0.075, 0.1 were carried out as follows. Polycrystalline samples of $(Pr_{1-y}Y_y)_{0.7}Ca_{0.3}CoO_3$ for $y = 0.0625$, 0.075, 0.1 were used whose transition temperatures at zero field are $T_C = 42, 64, 96$ K, respectively [10]. A nondestructive pulse magnet at the Institute for Solid State Physics, University of Tokyo, was used to generate pulsed magnetic fields of up to 50 T with 37-ms duration for the magnetization measurements using the induction method. The magnetization probe of the nondestructive pulse magnet was calibrated to the absolute value. Further, a horizontal-type single-turn coil (H-STC), a destructive pulse magnet at the Institute for Solid State Physics, University of Tokyo, was also used to generate magnetic fields of up to 140 T with 6-μs duration for the magnetization measurements using the induction method. In the case of the H-STC, the magnetization pickup coil consists of a pair of counterwound coils of 20 turns, either of which holds the sample inside [25]. The induction voltage $V_M \propto dM/dt$ was recorded with a digital oscilloscope. A He flow-type cryostat made of Bakelite was used to cool the sample down to 4.2 K. The temperature was monitored using a chromel-constantan thermocouple and a RuO_2 thermometer [18,26]. The induction voltage of the magnetic field $V_B \propto dB/dt$ was monitored at the position adjacent to the sample with a magnetic field pickup coil calibrated to the absolute value with a precision of $\sim$1%.

III. RESULT

Representative results of the measured V_M of $(Pr_{1-y}Y_y)_{0.7}Ca_{0.3}CoO_3$ with $y = 0.1$ at 18, 33, and 41 K and pulsed magnetic fields are shown in Fig. 1. First, the peaks in Fig. 1 indicated by arrows (b) and (c) indicate the steep increase and decrease of M in the ascending and descending magnetic fields, respectively. The peak positions and sharpness of the peaks in V_M are temperature dependent. Second, we note that the sharp peaks just after $t = 0$ μs indicated by arrow (a) in Fig. 1 are in good agreement with the observed magnetization increase below 1 T [27], which may originate in the Curie paramagnetism of Pr^{4+} or Co^{4+}, whose disappearance in the descending fields may be due to the heating effect. Third, each dM/dt curve commonly has a component proportional to dB/dt which shows little temperature dependence. A series of magnetization curves of $(Pr_{1-y}Y_y)_{0.7}Ca_{0.3}CoO_3$ is obtained by integrating V_M and is plotted for $y = 0.0625, 0.075, 0.1$ in Figs. 2(a)–2(c) as the thick black curves. Arrows pointing upwards and

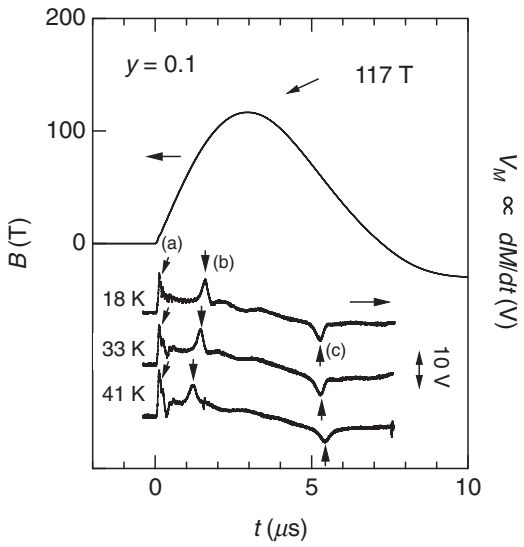

FIG. 1. Representative data of the induction voltage of the magnetization of $(Pr_{1-y}Y_y)_{0.7}Ca_{0.3}CoO_3$ ($y = 0.1$) and the pulsed magnetic field generated using the horizontal single-turn coils.

downwards indicate the magnetic transition fields in the ascending and descending fields, respectively. The absolute values for M obtained with the H-STC experiments are evaluated by fitting to the magnetization curves obtained using nondestructive pulses up to 50 T. As pointed out for the dM/dt curves in Fig. 1, we observed three components in the magnetization curves in Fig. 2. First, the sharp magnetic transitions are quite dependent on temperature and chemical pressure y because of their position and sharpness. The temperature-dependent magnetic transitions are attributed to the spin-state transition of Co^{3+}, which is the main focus of the following discussion. Second, the sudden increase and saturation of the magnetization below 10 T [27] may be attributed to the Curie paramagnetism of Pr^{4+} or Co^{4+}. The third component is the magnetization, which is proportional to the magnetic fields, showing little dependence on temperature. This component is considered to have other origins, such as the Van Vleck susceptibility of Pr^{4+} and Pr^{3+} because they are insensitive to temperature.

The heating effect during the magnetization process may not be as significant as it alters the understanding of the current data. For example, irreversible heating is expected in magnetization curves in Figs. 2(a)–2(c) due to the hysteresis loss [28]. The largest hysteresis loss is expected in the data at $y = 0.1$ and $T = 5$ K in Fig. 2(c). In this magnetization curve, we clearly observe the sharp first-order transition in both ascending and descending curves, which is not disturbed by the heating effect. On the other hand, for cases with $y = 0.075$ and 0.0625 at the lowest temperatures, the transitions in the descending curves are blurred compared with the ones in the ascending curves, although irreversible heating is expected to be smaller than that of $y = 0.1$ This observation indicates that the smearing effects in the descending curves observed for $y = 0.075$ and 0.0625 are not mainly due to the heating effects. We suspect dynamical effects leading to the sweep rate dependence are more relevant in the present case [23].

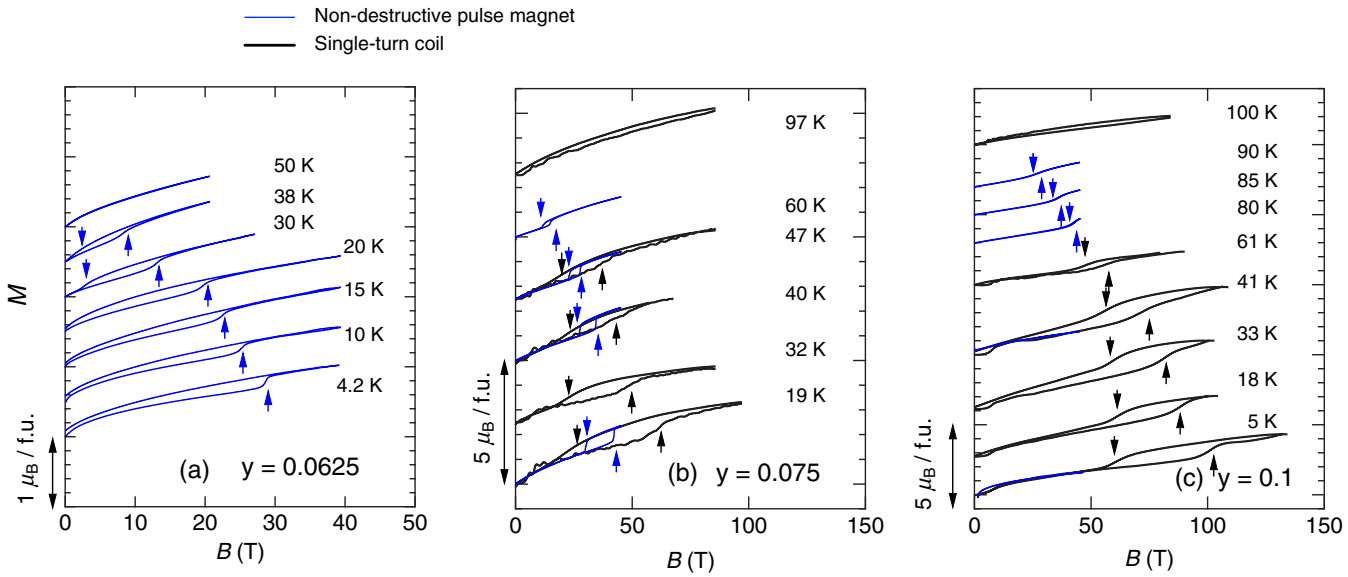

FIG. 2. Magnetization curves of $(Pr_{1-y}Y_y)_{0.7}Ca_{0.3}CoO_3$ for (a) $y = 0.0625$, (b) 0.075, and (c) 0.1, measured at various temperatures using the induction method.

We here define the mean transition fields as the average values of the magnetic transition fields in the ascending and descending fields in each magnetization curve in Fig. 2, which are calculated and plotted in the B-T-y space in Fig. 3. The magnetic transition fields coincide well with the transition fields of the metal-insulator transitions that were previously reported [22], as indicated by the open symbols in Fig. 3, suggesting strong coupling of the magnetism and conductivity in these systems up to ∼100 T. On the T-y plane at $B = 0$ T, in Fig. 3, the T-y phase diagram of $(Pr_{1-y}Y_y)_{0.7}Ca_{0.3}CoO_3$ is depicted according to the previous reports for $0 < y < 0.15$ [9,10]. At each y on the respective B-T plane, the ground state of the paramagnetic insular phase (PM/I) forms a domelike region, which is destroyed by either temperature or magnetic field. The region outside the nonmagnetic insulator phase is the paramagnetic metallic phase (PM/M), characterized by an increase in the magnetization and conductivity [22]. We specifically term the area colored in red in Fig. 3 the ferromagnetic metallic phase (FM/M) with spontaneous magnetization [9,10].

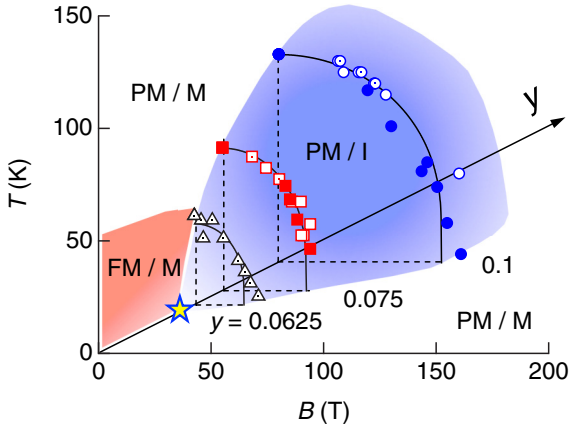

FIG. 3. Mean transition fields of $(Pr_{1-y}Y_y)_{0.7}Ca_{0.3}CoO_3$ obtained as a function of temperature and the amount of Y doping y. On the T-y plane at $B = 0$ T, the T-y phase diagram for $0 < y < 0.15$ is depicted based on Refs. [5,8,10]. Blue circles, red squares, and black triangles indicate transition fields for $y = 0.0625$, 0.075, and 0.1, respectively. Open symbols with a center dot indicate that they are obtained using nondestructive pulses. Open symbols without a dot indicate that they are obtained with resistivity measurements using the single-turn coil method adopted from Ref. [22]. Solid symbols indicate that they are obtained with inductive magnetization measurements using the single-turn coil method. Solid curves are the fittings to the data with the spin-crossover model.

IV. DISCUSSION

In the following discussion, we concentrate on the temperature-dependent features of the magnetization curves of $(Pr_{1-y}Y_y)_{0.7}Ca_{0.3}CoO_3$ for $y = 0.0625, 0.075, 0.1$, namely, the transition fields B_C (see Fig. 3) and the magnetization change ΔM [see Figs. 2 and 4(a)–4(c)] that are accompanied by the metal-insulator transition. First, we tentatively analyze the obtained B-T-y phase diagram (Fig. 3) and the magnetization curves with the spin-crossover model of a single ion based on Biernacki and Clerjaud's formulation [29], which is shown to give qualitative agreement with the experimental results. However, the experimentally obtained y dependence of ΔM does not agree with the model calculation, especially when approaching low temperatures. It is discussed that the discrepancy may arise from the itinerant magnetism of the paramagnetic metallic phase. Further, it is noted that a critical point may be present at low temperature and zero magnetic field with y slightly smaller than 0.0625. Last, we note the apparent contrast of the present phase diagram to that of $LaCoO_3$ and discuss the difference in the microscopic origins of those ground states.

The spin-crossover model used here is based on Biernacki and Clerjaud's formulation [29], where the Boltzmann distribution on a level scheme of a single-ion spin gap is

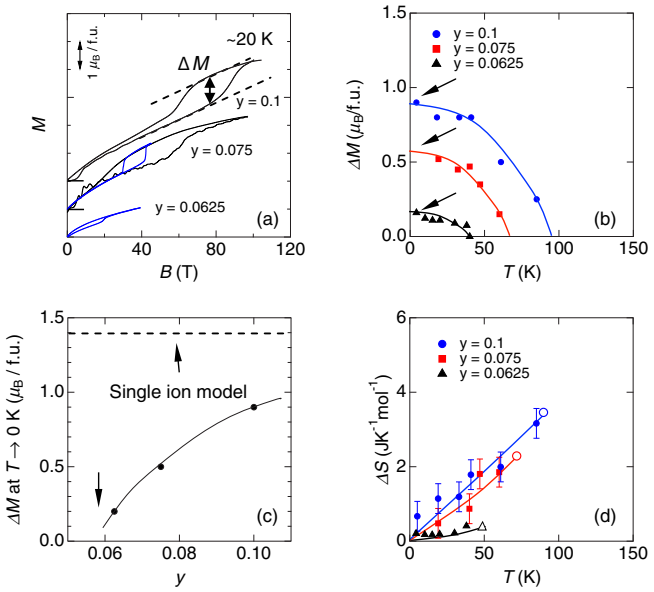

FIG. 4. (a) Magnetization curves of $(Pr_{1-y}Y_y)_{0.7}Ca_{0.3}CoO_3$ at ~20 K selected from Fig. 1. (b) The magnetization increase at the magnetic transition as a function of temperature. (c) The extrapolated magnetization increase at $T = 0$ K deduced in (b). (d) Increase of entropy ΔS at the magnetic transition deduced based on the Clausius-Clapeyron relation. The open symbols are reported data measured with heat-capacity measurements at $B = 0$ T as summarized in Table I. Solid curves in (b), (c), and (d) are guides for eyes.

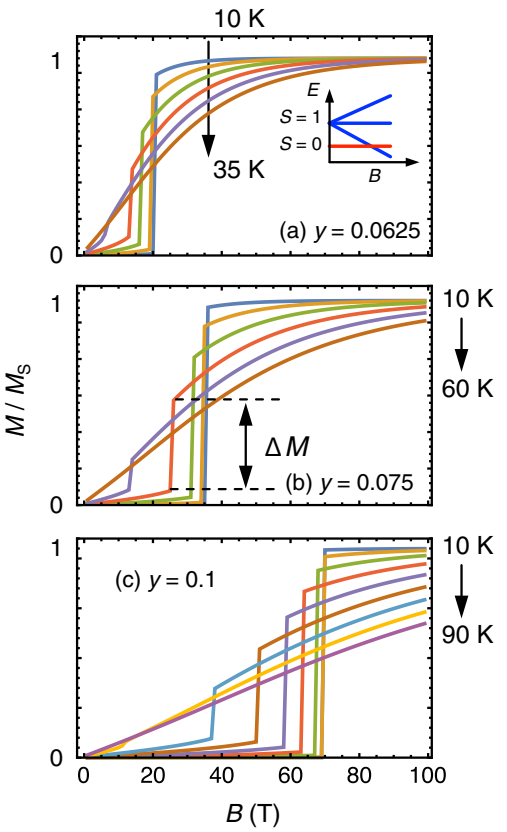

FIG. 5. Simulated magnetization curves based on the spin-crossover model of a single ion based on Biernacki and Clerjaud's formulation [29].

considered with further modification by mean fields of interion interactions (see the Appendix for details). The calculated B_C as a function of T using Eq. (A6) (solid curves in Fig. 3) are well fitted to the experimentally obtained transition fields assuming effective crystal-field splitting Δ' of 40, 70, 102 K with g factors of 2.7,2.8,2.1 for $y = 0.0625$, 0.075, 0.1, respectively. The increase in Δ' with increasing y is understood as the increase of crystal-field splitting with increasing chemical pressure. The simulated M shown in Fig. 5 calculated using $M = -\partial F/\partial B$ with Eq. (A5) are in qualitative agreement with the experimental results (Fig. 2), where B_C and ΔM increase with decreasing temperature or increasing y (chemical pressure corresponding here to increasing Δ'). However, when approaching low temperatures, striking discrepancies in M between the model calculation and the experimental observation are seen. In the calculated results, ΔM always converges to the saturation magnetization, as shown in Fig. 5 and summarized in Fig. 4(b). This is because the temperature dependence of ΔM in this model originates in the thermal smearing, which become negligible at low temperatures. In contrast, the experimentally obtained ΔM converge to values at low temperatures and decrease with decreasing y, as seen in Fig. 2 and summarized in Figs. 4(a)–4(c). In Fig. 4(c), ΔM of $1.4\mu_B$/f.u. at a temperature close to 0 K is estimated based on the single-ion model where the spin state of $0.7Co^{3+}$ changes from LS ($S = 0$) to IS ($S = 1$) with a g factor of 2. The estimated ΔM is independent of y, which highlights well the deviation from the experimentally obtained ΔM, which is largely y dependent.

Possible origins of the y dependence of ΔM are (i) a valence change of the Pr ion [27], (ii) the inhomogeneous spin-glass behavior of IS Co^{3+}, as seen in $La_{1-x}Sr_xCoO_3$ with $0 < x \leqq 0.18$ [30], and (iii) itinerant magnetism of Co in analogy to the cases of $La_{1-x}Sr_xMnO_3$ with $0.2 \leqq x \leqq 0.4$ [31] and $La_{1-x}Sr_xCoO_3$ with $x > 0.3$ [7,32].

First, the valence change of Pr ions during the phase transition is discussed as a possible origin of the y dependence of ΔM. We find below that the y dependence of the valence change is too small to account for the y dependence of the magnetization change in the region of y from 0.0625 to 0.1. In the crystal field of $(Pr_{1-y}Y_y)_{0.7}Ca_{0.3}CoO_3$, it is estimated that the $^3H_4$ multiplet of Pr^{3+} ($4f^2$) is split into nine nonmagnetic singlets and that the magnetism of the ground state is represented by an average Van Vleck susceptibility of $\chi = 0.018$ emu mol^{-1} Oe^{-1} [33]. As for Pr^{4+} ($4f^1$), the $^2F_{5/2}$ multiplet splits into three energetically well separated Kramers doublets (>32 meV), whose ground doublet is characterized by an anisotropic g factor of $g_x = 3.757$, $g_y = 0.935$, $g_z = 0.606$ [34]. Considering that the ground states are singlet and doublet for Pr^{3+} and Pr^{4+}, respectively, the magnetic field will stabilize Pr^{4+} rather than Pr^{3+}, inducing the valence change in the direction of Pr^{3+} to Pr^{4+}.

On the other hand, if the crystal-field effect is overwhelmed by the Zeeman effect at sufficiently high magnetic fields, it is possible that the moment of Pr^{3+} becomes larger than that

of Pr^{4+} due to the alternation of the ground state. In fact, there are excited singlets at 4.5, 14.5, and 16.0 meV above the ground singlet in Pr^{3+} ($4f^2$) [33] that will be transformed into magnetic eigenstates under ultrahigh magnetic fields. To roughly estimate the magnetic moments of Pr^{3+} and Pr^{4+} at high magnetic fields, we compare the magnetic moments of free ions. In this case, the $^3H_4$ multiplet of Pr^{3+} ($g_J = 4/5$) has a larger moment of $16/5\mu_B$ than the $^2F_{5/2}$ ($g_J = 6/7$) multiplet of Pr^{4+}, which has a moment of $15/7\mu_B$. It is then possible that the valence change in the direction of Pr^{4+} to Pr^{3+} drives the field-induced transition. If this is the case, the observed y dependence may be explained as the number of Pr ions that undergo the valence transition from 4+ to 3+. In the case of the thermally induced phase transition in $(Pr_{1-y}Y_y)_{0.7}Ca_{0.3}CoO_3$, the variation in the amount of the valence change in this y range is small as $\Delta v = 0.17$, 0.19, 0.2 for $y = 0.0625$, 0.075, 0.1, respectively [27,35]. Therefore, it is difficult to ascribe the observed y-dependent ΔM directly to the valence transition of Pr ions from 4+ to 3+.

Second, we discuss that the inhomogeneous spin-glass behavior of Co moments is unlikely to be the origin of the observed y-dependent magnetization change at low temperatures. In $La_{1-x}Sr_xCoO_3$ at $x < 0.18$, the inhomogeneous spin-glass behavior is observed [3,36]. If the solid is inhomogeneously magnetized in the field-induced spin-state transition, the value of ΔM may be proportional to the number of the Co ions that undergo the spin-state transition. In the spin-glass regime, the system remains insulating with a percolation limit of $x = 0.18$ [37]. If x is greater than 0.18, the ferromagnetic drop forms network, and the system becomes a homogeneous metal [11]. In the present case of $(Pr_{1-y}Y_y)_{0.7}Ca_{0.3}CoO_3$, all magnetic transitions are accompanied by the metal-insulator transition [22] even at $y = 0.0625$, where ΔM is only $0.2\mu_B$/f.u. [21,38], indicating the system is uniformly metallic above B_C or T_C. Therefore, the idea of inhomogeneous occupation of the magnetic spin states in $(Pr_{1-y}Y_y)_{0.7}Ca_{0.3}CoO_3$ in the metallic phase is not well supported.

Third, we consider the possibility where the magnetization of the paramagnetic metallic phase is determined by the itinerant magnetism of the Co^{3+} band. As noted in Ref. [6], the phase transition of $(Pr_{1-y}Y_y)_{0.7}Ca_{0.3}CoO_3$ with decreasing temperature is analogous to the virtual transition from the ferromagnetic metal $La_{1-x}Sr_xCoO_3$ to the diamagnetic insulator $LaCoO_3$. The double-exchange mechanism with Co^{3+} in the IS state is considered in play to form the ferromagnetic metallic phase in both $La_{1-x}Sr_xCoO_3$ with $x > 0.3$ and $La_{1-x}Sr_xMnO_3$ with $0.2 \leqq x \leqq 0.4$ [7,31,32]. The ferromagnetism in $La_{1-x}Sr_xCoO_3$ is considered to be characteristic, compared to the typical double-exchange system of $La_{1-x}Sr_xMnO_3$. The ferromagnetic moment of $La_{1-x}Sr_xCoO_3$ is smaller than its saturation moment, whereas in $La_{1-x}Sr_xMnO_3$ the saturation moment is achieved. It was discussed that this difference arises from the fact that $La_{1-x}Sr_xCoO_3$ has larger d-p hybridization with better itinerancy, evidenced by the sharper Fermi edge than in the case of $La_{1-x}Sr_xMnO_3$ [31], and the fact that $La_{1-x}Sr_xCoO_3$ is not a typical ferromagnet with a double-exchange mechanism but a more itinerant ferromagnet [7,32].

In the present case of $(Pr_{1-y}Y_y)_{0.7}Ca_{0.3}CoO_3$, we observed increasing ΔM with increasing chemical pressure y [Figs. 4(a), 4(b), and 4(c)]. For $(Pr_{1-y}Y_y)_{0.7}Ca_{0.3}CoO_3$, the pressure mainly affects the bond length and does not alter the bond angles of Co-O-Co [8]. With increasing pressure, therefore, the strength of d-p hybridization is expected to increase, which results in transforming the system from being similar to $La_{1-x}Sr_xMnO_3$ to being similar to $La_{1-x}Sr_xCoO_3$. This will cause a decrease in ΔM with increasing y, which is in disagreement with the observation. We note that the observed large chemical pressure dependence of the magnetization in the paramagnetic metal phase is not similar to previous double-exchange systems where less significant pressure effects are observed [39–42].

Rather, it appears more plausible to consider the Stoner model, where exchange splitting of the band is determined by the strength of the exchange interaction. In the present case, the origin of the exchange interaction is the double-exchange mechanism $J \propto t_0 \cos(\theta/2)$, where t_0 and θ are the transfer integral and relative angle of spins at adjacent sites. By applying pressure, t_0 is increased by stronger hybridization, resulting in the larger exchange interactions. This will lead to the enhanced exchange splitting of the spin bands. This idea is consistent with the observed y dependence of ΔM.

Here, we note the possible existence of the critical point at low temperatures in Fig. 3. One may notice that ΔM at $T \to 0$ K becomes negligibly small with decreasing y, as seen in Fig. 4(c), indicating that the second-order phase transition is realized at y slightly smaller than 0.0625. This trend is also the case for the values of ΔS at $B = 0$ T reported for heat-capacity measurements, as shown in Table I. It is therefore worth noting the possible existence of the critical point near the star in Fig. 3. The possible critical point separates the ferromagnetic metallic phase and the paramagnetic insulating phase. It is located at a very low temperature. Therefore, it may be important to consider the ferromagnetic fluctuation, the fluctuation between itineracy and localization, and the emerging quantum criticality in the adjacent region. We note that the possible critical point can be explored by varying the applied pressure on the samples with $y < 0.0625$.

We further estimated the chemical pressure y dependence of the latent heat at the temperature-induced phase transitions, which is defined as the enthalpy change $\Delta H_{B=0\ \mathrm{T}}$. $\Delta H_{T\to 0\ \mathrm{K}}$ at the magnetic-field-induce phase transitions is also calculated. Enthalpy of the magnetic system is defined as

$$\Delta H = T\Delta S + B\Delta M. \quad (1)$$

Equation (1) is reduced to $\Delta H_{B=0\ \mathrm{T}} = T_C\Delta S$ and $\Delta H_{T\to 0\ \mathrm{K}} = B_C\Delta M$ under respective conditions. We estimated each value of ΔH based on the reported values of T_C and ΔS at $B = 0$ T and the obtained values of ΔM and B_C at $T \to 0$ K, respectively. The results are summarized in Table I. The vanishingly decreasing latent heat with decreasing y directly indicates the change from the first-order phase transition to the second-order phase transition. The value of $\Delta H_{T\to 0\ \mathrm{K}}$ also becomes negligibly small, in good agreement with the above result. This trend is not reproduced in the estimated crystal-field gap Δ' in the spin-crossover model.

Last, we note that the obtained phase diagram has the domelike structure near its ground state, indicating that

TABLE I. Amount of Y doping y, transition temperature T_C at $B = 0$ T, change of entropy ΔS at $B = 0$ T, deduced enthalpy change $\Delta H_{B=0\ \mathrm{T}} = T_C \Delta S$, transition field B_C at $T \to 0$ K, change of magnetization ΔM at $T \to 0$ K, deduced enthalpy change $\Delta H_{T\to 0\ \mathrm{K}} = B_C \Delta M$, and crystal-field gap $\Delta' = T_C \ln 3$ used in the spin-crossover model.

y	T_C (K)	ΔS (J/K mol)	$\Delta H_{B=0\ \mathrm{T}}$ (K/f.u.)	B_C (T)	ΔM (μ_B/f.u.)	$\Delta H_{T\to 0\ \mathrm{K}}$ (K/f.u.)	Δ' (K/f.u.)
0.0625	40[a]	0.28[b]	1.35	17	0.15	2.55	44
0.075	64[a]	2.17[c]	16.7	40	0.51	20.4	70.3
0.1	93[a]	3.6[d]	41.6	80	0.9	72	102
0.15	132[a]	4.78[c]	75.9				

[a]Reference [27].
[b]Reference [21].
[c]Reference [35].
[d]Reference [43].

the low-entropy phase is at its ground state (Fig. 3). The entropy change at the field-induced phase transitions ΔS is also quantitatively deduced, as shown in Fig. 4(d) using the Clausius-Clapeyron relation, $dB/dT = -\Delta S/\Delta M$, and the experimentally obtained dB/dT in Fig. 3 and ΔM in Fig. 4(b). However, in $LaCoO_3$ the high magnetic-field-induced phase has a phase boundary with positive slope at $B > 100$ T, indicating that the low-entropy ordered phase is at the high magnetic-field-induced phase [18], which is strikingly different from the present case. The obtained phase diagram in Fig. 3 and the entropy change ΔS for $(Pr_{1-y}Y_y)_{0.7}Ca_{0.3}CoO_3$ in the present study show quite obvious contrasts to those obtained for $LaCoO_3$ in the previous study [18]. The difference between the phase diagrams of $(Pr_{1-y}Y_y)_{0.7}Ca_{0.3}CoO_3$ and $LaCoO_3$ may suggest the difference in the microscopic nature of the phase transition.

Recently, excitonic condensation was proposed to be realized in systems with the spin-state degree of freedom to account for the unusual insulating phase in the Pr-based perovskite cobalt family and $LaCoO_3$ [12–14]. More recently, Sotnikov and Kuneš and Tatsuno *et al.* independently claimed the possibility for the magnetic-field-induced excitonic condensation [19,20] to account for the recently found high-field phases of $LaCoO_3$ [18]. Tatsuno *et al.* claimed that in the case of $LaCoO_3$ the field-induced phase transition takes place in succession as LS → excitonic condensation (EC) → LS/HS → EC → HS phases [20]. Then, one fascinating and a consistent picture describing the B-T phase diagrams of $LaCoO_3$ and $(Pr_{1-y}Y_y)_{0.7}Ca_{0.3}CoO_3$ may be that $LaCoO_3$ is LS at its ground state, whereas $(Pr_{1-y}Y_y)_{0.7}Ca_{0.3}CoO_3$ is in the EC phase at its ground state. The theoretical suggestion that both LS and EC can be destroyed by the magnetic field may explain the field effects for both materials. Further experimental verification is needed to test those theories.

V. CONCLUSION

We have carried out the magnetization measurements of $(Pr_{1-y}Y_y)_{0.7}Ca_{0.3}CoO_3$ with $y = 0.0625$, 0.075, 0.1 at high magnetic fields up to 140 T and observed the magnetic phase transition. The B-T phase diagram obtained from the temperature dependence and the chemical pressure dependence of the transition fields is in good agreement with the single-ion model experiencing the spin crossover, where the ground state is the low-entropy phase. This is in contrast to the case of the previously investigated $LaCoO_3$ [18]. where the low-entropy ordered phase emerges at high magnetic fields. On the other hand, the qualitative discrepancy in the magnetization jump ΔM as a function of y in experiment and the single-ion model has been found. The origin of the discrepancy is attributed to the itinerant magnetism of the Co ion. Further, the existence of the critical point at low temperature is indicated by the vanishingly small ΔM, ΔS, and latent heat for decreasing y at low temperatures.

ACKNOWLEDGMENTS

The authors acknowledge J. Nasu and S. Ishihara for fruitful discussions, T. Nomura and Y. Kohama for useful comments, and K. Kindo and S. Takeyama for experimental support. This work was supported by JSPS KAKENHI Grant-in-Aid for Young Scientists (B) Grant No. 16K17738.

APPENDIX: A FIELD-INDUCED SPIN-CROSSOVER MODEL

The spin-crossover model of a single ion formulated by Biernacki and Clerjaud [29], where the spin crossover between LS and IS is induced by temperature or magnetic field and whose energy diagram is schematically shown in the inset of Fig. 5(a), is simplified and summarized below. The interion interactions are taken into account under the mean-field approximation. The interion interactions are effectively expressed by the elastic lattice model [44]. In the elastic lattice model, the energies of the LS and IS states are expressed as

$$E_{\mathrm{LS}} = \epsilon n^2, \tag{A1}$$

$$E_{\mathrm{IS}} = \Delta - g\mu_B B S_z + \epsilon(n-1)^2, \tag{A2}$$

where k, β, g, μ_B, Δ, S_z, and ϵ are the Boltzmann constant, $(kT)^{-1}$, the g factor, the Bohr magneton, the crystal-field gap, spin angular momentum in the z direction, and the elastic constant of the lattice, respectively. n is the increment of the lattice constant a normalized as $n = \Delta a/(a_{\mathrm{IS}} - a_{\mathrm{LS}})$, where a_{LS} and a_{IS} are the lattice constants when all Co ions are in the LS state and IS state and $\Delta a = a - a_{\mathrm{LS}}$, respectively; $n = 0$ and 1 correspond to the state of lattice with uniformly occupied LS states and IS states, respectively. According to Ref. [29], we can consider ϵ to be proportional to the interion interaction for the LS-LS or IS-IS pair. In this model we note

that n is also regarded as the occupancy of the IS state [29,44]. Specifically, when $\epsilon > 0$, the effective interactions for LS-LS and IS-IS pairs are attractive, and that for the IS-LS pair is repulsive, giving rising to the first-order spin-state transition at finite temperature. Thus, the partition function per single particle and n can be defined as

$$Z = \exp(-\beta E_{\mathrm{LS}}) + \sum_{S_z=1,0,-1} \exp(-\beta E_{\mathrm{IS}}), \tag{A3}$$

$$n = \frac{\sum_{S_z=1,0,-1} \exp(-\beta E_{\mathrm{IS}})}{Z}, \tag{A4}$$

respectively. The one-particle free energy is obtained as $F = -\beta^{-1} \ln Z$. Then, we obtain the equilibrium value of n by obtaining the minimum of F as

$$\frac{\partial F}{\partial n} = 0, \tag{A5}$$

with the condition of $\partial^2 F/\partial n^2 > 0$. The transition fields as a function of temperature $B_{\mathrm{C}}(T)$ can be obtained by numerically solving Eq. (A5) with the condition $n = 1/2$ as [29]

$$T_{\mathrm{C}} = \frac{\Delta'}{k \ln P}, \tag{A6}$$

where $\Delta' = \Delta - \epsilon$ and

$$P = \frac{\sinh\{\beta(2s+1)g\mu_{\mathrm{B}} B_{\mathrm{C}}/2\}}{\sinh(\beta g \mu_{\mathrm{B}} B_{\mathrm{C}}/2)}, \tag{A7}$$

where we take $s = 1$ for IS. At $B = 0$ T, Eqs. (A6) and (A7) reduce to the form $T_{\mathrm{C}} = \Delta'/\{k \ln(2s+1)\}$. At $T = 0$ K, on the other hand, Eqs. (A6) and (A7) reduce to the form $B_{\mathrm{C}} = \Delta'/(g\mu_{\mathrm{B}} s)$. Both forms are readily understandable and useful for estimating Δ' and g.

[1] K. Asai, O. Yokokura, N. Nishimori, H. Chou, J. M. Tranquada, G. Shirane, S. Higuchi, Y. Okajima, and K. Kohn, Phys. Rev. B **50**, 3025 (1994).

[2] T. Saitoh, T. Mizokawa, A. Fujimori, M. Abbate, Y. Takeda, and M. Takano, Phys. Rev. B **55**, 4257 (1997).

[3] P. M. Raccah and J. B. Goodenough, Phys. Rev. **155**, 932 (1967).

[4] M. A. Korotin, S. Y. Ezhov, I. V. Solovyev, V. I. Anisimov, D. I. Khomskii, and G. A. Sawatzky, Phys. Rev. B **54**, 5309 (1996).

[5] S. Tsubouchi, T. Kyômen, M. Itoh, P. Ganguly, M. Oguni, Y. Shimojo, Y. Morii, and Y. Ishii, Phys. Rev. B **66**, 052418 (2002).

[6] K. Knížek, J. Hejtmánek, P. Novák, and Z. Jirák, Phys. Rev. B **81**, 155113 (2010).

[7] T. Saitoh, T. Mizokawa, A. Fujimori, M. Abbate, Y. Takeda, and M. Takano, Phys. Rev. B **56**, 1290 (1997).

[8] T. Fujita, T. Miyashita, Y. Yasui, Y. Kobayashi, M. Sato, E. Nishibori, M. Sakata, Y. Shimojo, N. Igawa, Y. Ishii, K. Kakurai, T. Adachi, Y. Ohishi, and M. Takata, J. Phys. Soc. Jpn. **73**, 1987 (2004).

[9] S. Tsubouchi, T. Kyômen, M. Itoh, and M. Oguni, Phys. Rev. B **69**, 144406 (2004).

[10] T. Naito, H. Sasaki, and H. Fujishiro, J. Phys. Soc. Jpn. **79**, 034710 (2010).

[11] D. Phelan, K. P. Bhatti, M. Taylor, S. Wang, and C. Leighton, Phys. Rev. B **89**, 184427 (2014).

[12] J. Kuneš and P. Augustinský, Phys. Rev. B **90**, 235112 (2014).

[13] T. Kaneko, K. Seki, and Y. Ohta, Phys. Rev. B **85**, 165135 (2012).

[14] J. Nasu, T. Watanabe, M. Naka, and S. Ishihara, Phys. Rev. B **93**, 205136 (2016).

[15] K. Sato, A. Matsuo, K. Kindo, Y. Kobayashi, and K. Asai, J. Phys. Soc. Jpn. **78**, 093702 (2009).

[16] M. M. Altarawneh, G. W. Chern, N. Harrison, C. D. Batista, A. Uchida, M. Jaime, D. G. Rickel, S. A. Crooker, C. H. Mielke, J. B. Betts, J. F. Mitchell, and M. J. R. Hoch, Phys. Rev. Lett. **109**, 037201 (2012).

[17] M. Rotter, Z. S. Wang, A. T. Boothroyd, D. Prabhakaran, A. Tanaka, and M. Doerr, Sci. Rep. **4**, 7003 (2014).

[18] A. Ikeda, T. Nomura, Y. H. Matsuda, A. Matsuo, K. Kindo, and K. Sato, Phys. Rev. B **93**, 220401(R) (2016).

[19] A. Sotnikov and J. Kuneš, Sci. Rep. **6**, 30510 (2016).

[20] T. Tatsuno, E. Mizoguchi, J. Nasu, M. Naka, and S. Ishihara, J. Phys. Soc. Jpn. **85**, 083706 (2016).

[21] T. Naito, H. Fujishiro, T. Nishizaki, N. Kobayashi, J. Hejtmánek, K. Knížek, and Z. Jirák, J. Appl. Phys. **115**, 233914 (2014).

[22] S. Lee, Y. H. Matsuda, T. Naito, D. Nakamura, and S. Takeyama, J. Phys. Soc. Jpn. **84**, 044703 (2015).

[23] S. Kimura, Y. Narumi, K. Kindo, M. Nakano, and G.-e. Matsubayashi, Phys. Rev. B **72**, 064448 (2005).

[24] S. Kimura, Y. Maeda, T. Kashiwagi, H. Yamaguchi, M. Hagiwara, S. Yoshida, I. Terasaki, and K. Kindo, Phys. Rev. B **78**, 180403 (2008).

[25] S. Takeyama, R. Sakakura, Y. H. Matsuda, A. Miyata, and M. Tokunaga, J. Phys. Soc. Jpn. **81**, 014702 (2012).

[26] K. Amaya, S. Takeyama, T. Nakagawa, M. Ishizuka, K. Nakao, T. Sakakibara, T. Goto, N. Miura, Y. Ajiro, and H. Kikuchi, Phys. B (Amsterdam, Neth.) **155**, 396 (1989).

[27] J. Hejtmánek, Z. Jirák, O. Kaman, K. Knížek, E. Šantavá, K. Nitta, T. Naito, and H. Fujishiro, Eur. Phys. J. B **86**, 305 (2013).

[28] T. Nomura, Y. H. Matsuda, S. Takeyama, and T. C. Kobayashi, J. Phys. Soc. Jpn. **85**, 094601 (2016).

[29] S. W. Biernacki and B. Clerjaud, Phys. Rev. B **72**, 024406 (2005).

[30] M. Itoh, I. Natori, S. Kubota, and K. Motoya, J. Phys. Soc. Jpn. **63**, 1486 (1994).

[31] T. Saitoh, A. Sekiyama, K. Kobayashi, T. Mizokawa, A. Fujimori, D. D. Sarma, Y. Takeda, and M. Takano, Phys. Rev. B **56**, 8836 (1997).

[32] J. Okamoto, H. Miyauchi, T. Sekine, T. Shidara, T. Koide, K. Amemiya, A. Fujimori, T. Saitoh, A. Tanaka, Y. Takeda, and M. Takano, Phys. Rev. B **62**, 4455 (2000).

[33] P. Novák, K. Knížek, M. Maryško, Z. Jirák, and J. Kuneš, J. Phys. Condens. Matter **25**, 446001 (2013).

[34] Z. Jirák, J. Hejtmánek, K. Knížek, M. Maryško, P. Novák, E. Šantavá, T. Naito, and H. Fujishiro, J. Phys. Condens. Matter **25**, 216006 (2013).

[35] J. Hejtmánek, E. Šantavá, K. Knížek, M. Maryško, Z. Jirák, T. Naito, H. Sasaki, and H. Fujishiro, Phys. Rev. B **82**, 165107 (2010).

[36] S. Yamaguchi, H. Taniguchi, H. Takagi, T. Arima, and Y. Tokura, J. Phys. Soc. Jpn. **64**, 1885 (1995).

[37] S. Yamaguchi, Y. Okimoto, H. Taniguchi, and Y. Tokura, Phys. Rev. B **53**, R2926 (1996).

[38] M. Maryško, Z. Jirák, K. Knížek, P. Novák, J. Hejtmánek, T. Naito, H. Sasaki, and H. Fujishiro, J. Appl. Phys. **109**, 07E127 (2011).

[39] Y. Moritomo, A. Asamitsu, and Y. Tokura, Phys. Rev. B **51**, 16491 (1995).

[40] Y. Moritomo, H. Kuwahara, Y. Tomioka, and Y. Tokura, Phys. Rev. B **55**, 7549 (1997).

[41] R. Lengsdorf, M. Ait-Tahar, S. S. Saxena, M. Ellerby, D. I. Khomskii, H. Micklitz, T. Lorenz, and M. M. Abd-Elmeguid, Phys. Rev. B **69**, 140403 (2004).

[42] I. Fita, R. Szymczak, R. Puzniak, I. O. Troyanchuk, J. Fink-Finowicki, Y. M. Mukovskii, V. N. Varyukhin, and H. Szymczak, Phys. Rev. B **71**, 214404 (2005).

[43] J. Hejtmánek, Z. Jirák, O. Kaman, K. Knížek, E. Šantavá, K. Nitta, T. Naito, and H. Fujishiro (private communication).

[44] D. B. Chesnut, J. Chem. Phys. **40**, 405 (1964).